Development 140, 1970-1980 (2013) doi:10.1242/dev.088104

Anteroposterior and dorsoventral patterning are coordinated by an identical patterning clock

Megumi Hashiguchi and Mary C. Mullins*

SUMMARY

Establishment of the body plan in vertebrates depends on the temporally coordinated patterning of tissues along the body axes. We have previously shown that dorsoventral (DV) tissues are temporally patterned progressively from anterior to posterior by a BMP signaling pathway. Here we report that DV patterning along the zebrafish anteroposterior (AP) axis is temporally coordinated with AP patterning by an identical patterning clock. We altered AP patterning by inhibiting or activating FGF, Wnt or retinoic acid signaling combined with inhibition of BMP signaling at a series of developmental time points, which revealed that the temporal progression of DV patterning is directly coordinated with AP patterning. We investigated how these signaling pathways are integrated and suggest a model for how DV and AP patterning are temporally coordinated. It has been shown that in *Xenopus* dorsal tissues FGF and Wnt signaling quell BMP signaling by degrading phosphorylated (P) Smad1/5, the BMP pathway signal transducer, via phosphorylation of the Smad1/5 linker region. We show that in zebrafish FGF/MAPK, but not Wnt/GSK3, phosphorylation of the Smad1/5 linker region localizes to a ventral vegetal gastrula region that could coordinate DV patterning with AP patterning ventrally without degrading P-Smad1/5. Furthermore, we demonstrate that alteration of the MAPK phosphorylation sites in the Smad5 linker causes precocious patterning of DV tissues along the AP axis during gastrulation. Thus, DV and AP patterning are intimately coordinated to allow cells to acquire both positional and temporal information simultaneously.

KEY WORDS: Dorsoventral patterning, Anteroposterior patterning, BMP, Wnt, FGF, Retinoic acid, Temporal regulation, P-Smad, MAPK, GSK3

INTRODUCTION

A bone morphogenetic protein (BMP) signaling gradient patterns cells along the embryonic dorsoventral (DV) axis (Little and Mullins, 2006). BMP signaling is abrogated dorsally by the secreted BMP antagonists Chordin, Noggin and Follistatin to generate low BMP signaling levels that allow neurectodermal tissues to develop. These and additional extracellular modulators generate the moderate and high levels of BMP signaling that specify lateral and ventral cell types, respectively (Langdon and Mullins, 2011).

In addition to DV patterning of axial tissues, the embryo is also patterned along the anteroposterior (AP) and left-right axes. Although patterning of each of these axes has been well studied, little is known about how patterning is coordinated between each of these axes. We previously showed that DV tissues are patterned temporally progressively from anterior to posterior (Tucker et al., 2008). It is known that AP tissues are also patterned temporally progressively from anterior to posterior (Gamse and Sive, 2000; Gamse and Sive, 2001; Stern et al., 2006). However, it is not known if the patterning of DV and AP tissues is coordinated. Here we investigate whether the temporal patterning of DV and AP tissues is coordinated by the same patterning clock or occurs independently.

AP patterning is mediated by fibroblast growth factor (FGF), Wnt and retinoic acid (RA) posteriorizing signals during gastrulation (Gamse and Sive, 2000; Maden, 2002; Schier and Talbot, 2005; Stern et al., 2006; Wilson and Houart, 2004). To allow anterior neural tissues to develop, FGF and Wnt signaling must be repressed while these signals actively specify more posterior neural tissue development (Erter et al., 2001; Houart et al., 2002; Kudoh et al., 2004; Kudoh et al., 2002; Ramel et al., 2005; Rhinn et al., 2005; Shimizu et al., 2005). RA signaling does not posteriorize the most anterior neurectodermal tissues, but acts to posteriorize more caudal neural tissue (Kudoh et al., 2002; Maves and Kimmel, 2005). In zebrafish, expression of FGF, Wnt and RA signaling components overlap in the marginal zone (Schier and Talbot, 2005). In addition, the expression of these AP patterning components in the ventral marginal zone overlaps with that of BMP signaling components, suggesting the potential interaction of DV and AP patterning pathways during gastrulation.

In *Xenopus*, a model has been proposed to coordinate DV and AP patterning in dorsal tissues through integration of FGF and Wnt signaling into the BMP signaling pathway. Following phosphorylation by the BMP receptor, Smad1 is subsequently phosphorylated by FGF/MAPK and Wnt/GSK3, which leads to its degradation (Fuentealba et al., 2007). Although degradation of phosphorylated (P) Smad1/5 is not evident in ventral regions along the AP axis of the zebrafish gastrula (Tucker et al., 2008), a mechanism independent of P-Smad1/5 degradation might integrate BMP signaling with MAPK and GSK3 on P-Smad1/5 to coordinate DV and AP temporal patterning.

Here we demonstrate that patterning of DV tissues along the AP axis is intimately coordinated with AP patterning during zebrafish gastrulation. When FGF, Wnt or RA signaling pathways were inhibited in combination with the temporal modulation of BMP signaling, we found that patterning of DV tissues by BMP signaling along the AP axis is coordinated with AP patterning by FGF, Wnt and RA. Furthermore, our results suggest that coordinated patterning is regulated in part by phosphorylation of the P-Smad1/5 linker region via FGF/MAPK. The coordinated patterning of AP and DV tissues allows a cell to adopt both DV and AP positional information simultaneously during gastrulation.

Department of Cell and Developmental Biology, University of Pennsylvania, Perelman School of Medicine, 1211 BRBII/III, 421 Curie Blvd., Philadelphia, PA 19104-6058, USA.

*Author for correspondence (mullins@mail.med.upenn.edu)

Accepted 19 February 2013

MATERIALS AND METHODS

Fish strains

The mutant strain *somitabun*^{dtc24} (*sbn*, *smad5*) (Mullins et al., 1996; Nguyen et al., 2000), which contains a missense mutation in the MH domain (Hild et al., 1999), was used. All progeny of *sbn*^{dtc24} heterozygous females are mutant owing to the dominant maternal-effect nature of this mutation (Mullins et al., 1996). The transgenic lines Tg(*hsp70:chordin*) [Tg(*hsp70:chd*)] and Tg(*hsp70:dkk1GFP*) have been described (Stoick-Cooper et al., 2007; Tucker et al., 2008).

Pharmacological treatments

Zebrafish embryos were treated with 300 µM SU5402 (Mohammadi et al., 1997) (Calbiochem, TOCRIS) in E3 medium as described (Shimizu et al., 2005). RA (1 nM) and LiCl (300 mM) treatments were performed as described (Kudoh et al., 2002). DEAB (5 µM) treatment was performed as described (Maves and Kimmel, 2005). DMH1 (10 mM stock solution in DMSO; gift from C. Hong, Vanderbilt University) was diluted to 1 µM in E3 medium. As controls of DMH1, SU5402, DEAB and RA treatments, embryos were treated with equivalent concentrations of DMSO. Embryos retained their chorions during all treatments.

mRNA and morpholino injections

RNAs encoding synthetic human SMAD1 wild type (*hSmad1WT*) (250, 350 and 450 pg), SMAD1 mutated at the MAPK sites (*hSmad1MM*) (250, 350 and 450 pg) and SMAD1 mutated at the GSK3 sites (*hSmad1GM*) (350 pg) (Fuentealba et al., 2007) were synthesized using the mMessage mMachine Kit (Ambion). The RNAs were injected into one-cell stage embryos from an incross of homozygous Tg(*hsp70:chd*) fish or *sbn*^{dtc24}/+ fish. The sequences of *smad5* morpholino 1 and morpholino 3 (*smad5* MOs) are described (Schumacher et al., 2011). *smad5* MO1 and MO3 (3 ng each) were injected into Tg(*hsp70:chd*) embryos at the one-cell stage. *smad5* MOs and the above RNAs were injected using separate needles in double and single injections to control for the effectiveness of the MOs and RNAs.

In situ hybridization

In situ hybridization was performed as described using *gbx1* (Rhinn et al., 2003), *hoxb1a* (Prince et al., 1998), *hoxb1b* (Alexandre et al., 1996), *krox20* (Oxtoby and Jowett, 1993), *no tail* (Schulte-Merker et al., 1992), *otx2* (Li et al., 1994), *pax2.1* (*pax2a*) (Krauss et al., 1992) and *six3* (Kobayashi et al., 1998) probes.

Western blotting

Anti-P-Smad1/5 and anti-actin western blots were carried out as described (Schumacher et al., 2011). Anti-total Smad5 western blot was performed using the same conditions. Primary antibodies used were P-Smad1/5 (1:500, Cell Signaling Technology) and total Smad5 (1:1500, GeneTex).

Immunostaining

Immunostaining and confocal microscopy were performed as described (Tucker et al., 2008). Primary antibodies used were P-Smad1^{MAPK} [1:1250 (Fuentealba et al., 2007)], P-Smad1^{GSK3} [1:1000 (Fuentealba et al., 2007)] and total Smad5 antibody (1:100, GeneTex).

RESULTS

BMP signaling temporally patterns tissues progressively along the AP axis during blastula and gastrula stages

We began by examining the temporal patterning of DV tissues along the AP axis by BMP signaling during zebrafish blastula and gastrula stages. We inhibited BMP signaling at a series of time points using the transgene Tg(*hsp70:chd*) to drive expression of the *chordin* BMP antagonist with a heat shock-inducible promoter (Tucker et al., 2008). This transgene can inhibit all BMP activity and P-Smad1/5 within 60 minutes after the initiation of a 1-hour heat shock (HS) (Tucker et al., 2008). Following the HS treatments, we then investigated how DV tissues were affected along the AP axis by examining the expression of genes that mark distinct neurectodermal regions along this axis.

We found that a 1-hour HS of Tg(*hsp70:chd*) embryos at the 1000-cell stage [mid-blastula, 3.0 hours postfertilization (hpf)] caused expression of the prospective forebrain marker *six3* (Kobayashi et al., 1998) to expand fully to the ventral side (Fig. 1A,B), whereas HS at or after the high stage (3.3 hpf) showed normal localization of *six3* expression (Fig. 1C-F). HS at sphere (4 hpf) and 40% epiboly (late blastula, 5 hpf) stages caused expression of the forebrain and mid-brain marker *otx2* (Li et al., 1994; Mori et al., 1994) to expand to the ventral side, whereas HS at or after the 50% epiboly stage (5.3 hpf) led to normal *otx2* expression (Fig. 1G-L) (Tucker et al., 2008). HS at sphere, 40% and 50% epiboly stages resulted in expansion of the rostral hindbrain marker *gbx1* (Rhinn et al., 2003) fully to the ventral side (Fig. 1M-P), whereas expression was restricted to the dorsal side by HS at or after the shield stage (Fig. 1Q,R). Finally, expression of the caudal hindbrain marker *hoxb1b* (Alexandre et al., 1996) was expanded ventrally in embryos subject to HS at 40% epiboly, shield (6 hpf) and 65% epiboly (7 hpf) stages (Fig. 1S-V), whereas embryos with HS at or after 70% epiboly (7.5 hpf) displayed normal *hoxb1b* expression (Fig. 1W,X).

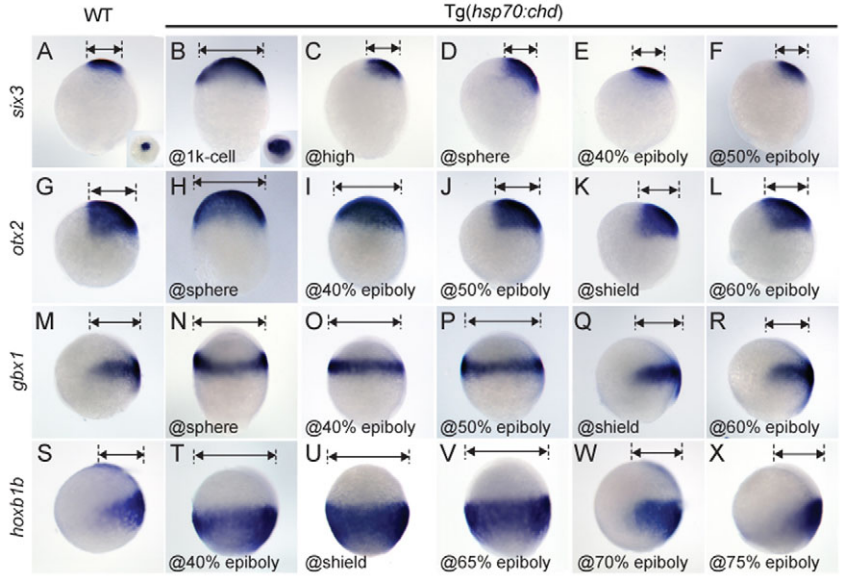

Fig. 1. Progressive DV neurectodermal patterning along the AP axis revealed by a Tg(*hsp70:chd*) BMP inhibition series. (**A-F**) *six3*, (**G-L**) *otx2* and (**M-R**) *gbx1* expression in anterior neurectoderm and (**S-X**) *hoxb1b* expression in posterior neurectoderm in non-heat shocked Tg(*hsp70:chd*) (WT) zebrafish embryos (A,G,M,S) and in Tg(*hsp70:chd*) embryos subject to heat shock (HS) at the indicated stages to inhibit BMP signaling (B-F,H-L,N-R,T-X). 1K-cell, 1000-cell stage. The DV width of the expression domain is indicated. Lateral views, dorsal to right, except for insets in A and B, which are animal pole views. (A-R) Shown at 80% epiboly stage; (S-X) shown at 90-95% epiboly stage. A, *n*=9/9; B, *n*=7/9; C, *n*=9/10; D, *n*=11/11; E, *n*=12/12; F, *n*=10/10; G, *n*=30/30; H, *n*=27/31; I, *n*=25/29; J, *n*=21/21; K, *n*=37/39; L, *n*=10/10; M, *n*=9/9; N, *n*=13/13; O, *n*=9/9; P, *n*=8/9; Q, *n*=9/10; R, *n*=10/10; S, *n*=32/32; T, *n*=26/27; U, *n*=21/22; V, *n*=28/29; W, *n*=17/20; X, *n*=20/21.

In Tg(*hsp70:chd*) embryos, P-Smad5 is greatly reduced 40 minutes after the start of HS and is absent by 60 minutes (Tucker et al., 2008). Thus, BMP signaling patterns each of the above AP tissue markers ~60 minutes after initiation of HS. Taken together, neurectodermal tissues from prospective forebrain to caudal hindbrain are patterned progressively over time from late blastula to late gastrula stages.

Temporal patterning of DV tissues is coordinated with AP patterning modulated by FGF signaling

Because the temporal patterning of AP tissues in vertebrates is known to occur progressively, we hypothesized that DV and AP patterning are coordinated by the same patterning clock. To test this hypothesis, we disrupted AP patterning by inhibiting or activating FGF, Wnt or RA signaling pathways and then determined how temporal patterning by BMP signaling was affected. If DV and AP patterning are coordinated, we would expect that alterations in AP patterning would effect similar alterations in the temporal patterning of DV tissues. For example, in anteriorized embryos, i.e. those showing a loss of posterior tissue with a concomitant expansion of anterior tissue (located in a more caudal position of the embryo; red dashed line in Fig. 2A, upper panels), the caudally expanded anterior tissue would be patterned with the normal anterior domain timing, rather than when the more caudal domain is normally patterned by BMP signaling (Fig. 2A, model 1). Conversely, if DV patterning instead proceeds by a distinct temporal patterning mechanism, then alterations in AP patterning will not affect the progressive temporal patterning of DV tissues by BMP signaling. For example, in anteriorized embryos, the caudally expanded anterior tissue would be patterned at a later time point when the more posterior tissue is normally patterned, i.e. the temporal progression of BMP patterning would not be altered by changes in AP patterning and would progress normally (Fig. 2A, model 2).

To examine whether DV patterning is coordinated with AP patterning, we inhibited FGF signaling, a posteriorizing signal, in combination with temporally inhibiting BMP signaling. FGF signaling was inhibited with SU5402, a specific FGF receptor inhibitor (Fürthauer et al., 2004; Mohammadi et al., 1997). Because FGF signaling also functions in DV patterning during blastula stages (Fürthauer et al., 2004; Maegawa et al., 2006), we treated embryos with SU5402 beginning at shield stage (early gastrula stage), which we found caused a specific AP patterning defect without altering DV patterning. Anteriorization was evident by examining the anterior neurectodermal marker *otx2* in late gastrula. Inhibition of FGF signaling caused *otx2* expression to expand posteriorly, but not ventrally (Fig. 2B,G) (Kudoh et al., 2004). Inhibition of BMP signaling by HS of Tg(*hsp70:chd*) embryos at sphere (4 hpf) and 40% epiboly (late blastula, 5 hpf) stages caused *otx2* expression to expand ventrally (Fig. 2C,D) (Tucker et al., 2008). Embryos with HS at or after 50% epiboly (5.3 hpf) displayed normal *otx2* expression (Fig. 2E,F) (Tucker et al., 2008).

We then examined whether BMP signaling patterns the caudally expanded anterior tissue when these anterior tissues are normally patterned or at a later time point corresponding to its new more caudal location. We treated Tg(*hsp70:chd*) embryos with SU5402 to anteriorize the tissue, followed by a series of HSs to determine when BMP signaling patterns the expanded anterior tissue. We found that the expanded anterior tissue (Fig. 2H-K) was patterned during the same temporal interval as the normally positioned anterior tissue (Fig. 2C-F). These results suggest that temporal DV patterning by BMP signaling along the AP axis is coordinated with AP patterning mediated by FGF signaling.

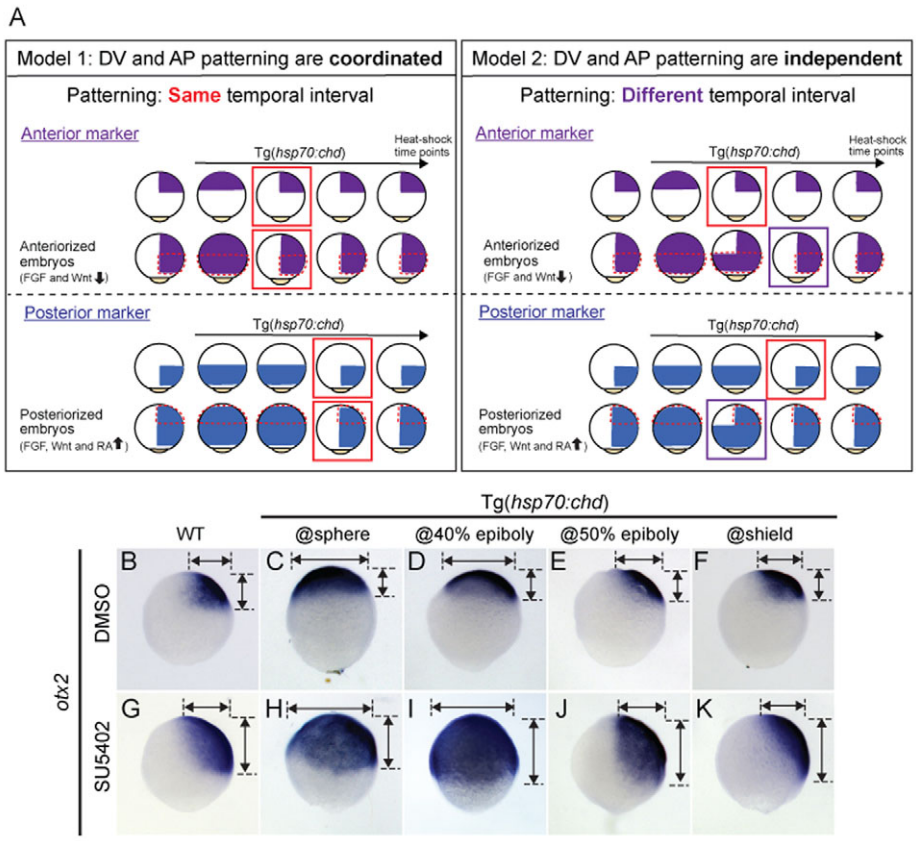

Fig. 2. Models of coordinate and independent DV and AP patterning, and anteriorization by FGF inhibition is patterned by BMP signaling with the same temporal dynamics as the normal domain. (**A**) Models in which DV and AP patterning are coordinated (model 1) or independent (model 2). Embryos are represented at late gastrula stage. The red dashed lines indicate the posteriorly expanded anterior tissue in the top panels and the anteriorly expanded posterior tissue in the bottom panels. (**B-K**) *otx2* expression in anterior neurectoderm in non-heat shocked Tg(*hsp70:chd*) zebrafish embryos (WT) (B,G) and following HS at the indicated stages (C-F,H-K), with (G-K) or without (B-F) inhibition of FGF signaling by SU5402. The DV width and the AP length of *otx2* expression are indicated by horizontal and vertical arrows, respectively. Lateral views, dorsal to right, at 80% epiboly. B, *n*=30/30; C, *n*=27/31; D, *n*=25/29; E, *n*=21/21; F, *n*=37/39; G, *n*=37/39; H, *n*=34/37; I, *n*=37/40; J, *n*=23/25; K, *n*=34/35.

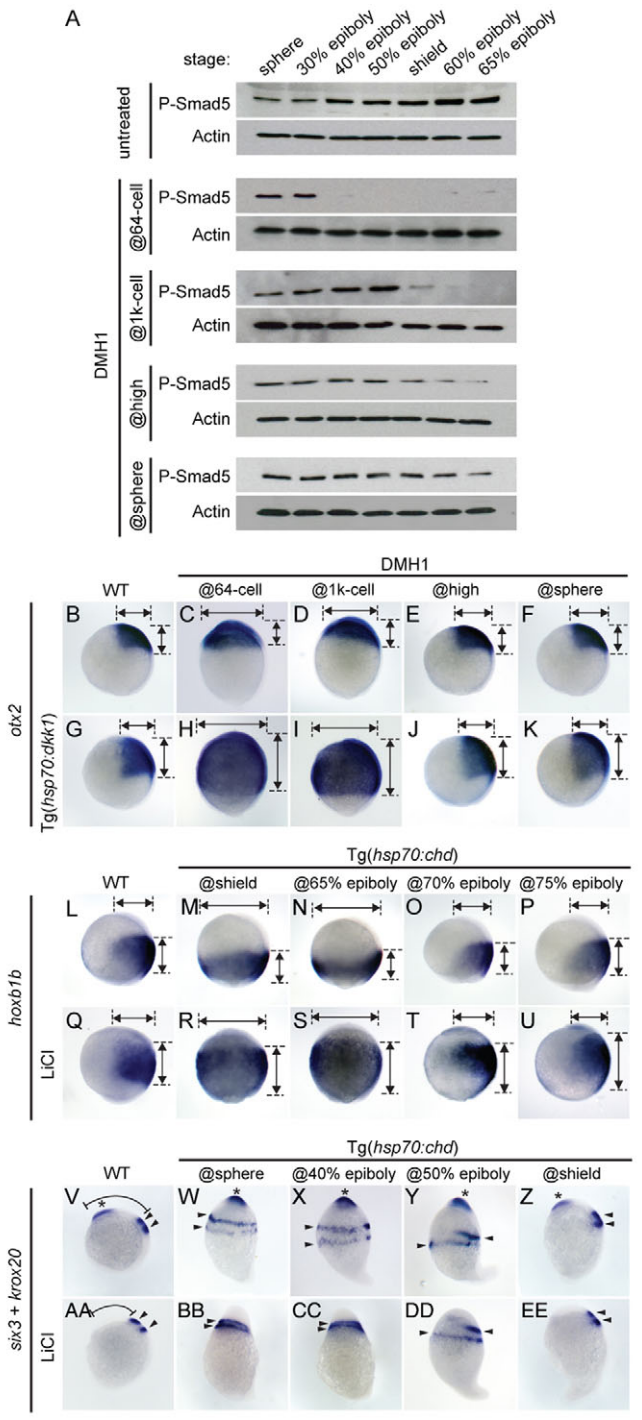

Fig. 3. Temporal effectiveness of DMH1 in inhibiting P-Smad1/5, and the temporal patterning dynamics of DV tissues are unchanged when posteriorized or anteriorized by altered Wnt signaling. (**A**) P-Smad5 western blot for embryos collected at the indicated stages after treatment with the BMP signaling inhibitor DMH1 at the 64-cell, 1000-cell, high and sphere stages. Actin is a loading control. (**B-K**) Expression of *otx2* in untreated wild type (B) and in wild type treated with DMH1 at the indicated stages (C-F). *otx2* expression in HS Tg(*hsp70:dkk1*) embryos without (G) and with DMH1 treatment at the indicated stages (H-K). (**L-U**) Expression of *hoxb1b* in Tg(*hsp70:chd*) embryos not subject to HS (WT) (L,Q) and subject to HS at the indicated stages (M-P,R-U), without (L-P) and with (Q-U) LiCl treatment to activate Wnt signaling and posteriorize the embryos. (**V-EE**) Expression of *six3* (asterisk) and *krox20* (arrowheads) in wild type (V,AA) and in Tg(*hsp70:chd*) embryos subject to HS at the indicated stages (W-Z,BB-EE), without (V-Z) and with (AA-EE) LiCl treatment. The distance from the anterior tip of the head to the anterior boundary of r3 is indicated (V,AA). LiCl treatment was at shield stage. HS of Tg(*hsp70:dkk1*) embryos was performed at 37°C for 1 hour from 50% epiboly stage (5.3 hpf) to shield stage (6 hpf). Lateral views, dorsal to right. Embryos are shown at (B-K) 80% epiboly, (L-U) 90% epiboly and (V-EE) 6-somite stage. B, *n*=10/10; C, *n*=18/19; D, *n*=17/18; E, *n*=16/16; F, *n*=16/16; G, *n*=16/21; H, *n*=17/23; I, *n*=16/22; J, *n*=18/20; K, *n*=17/21; L, *n*=18/18; M, *n*=16/19; N, *n*=16/18; O, *n*=18/19; P, *n*=16/17; Q, *n*=9/13; R, *n*=10/15; S, *n*=16/18; T, *n*=18/20; U, *n*=17/19; V, *n*=23/23; W, *n*=18/19; X, *n*=16/18; Y, *n*=13/16; Z, *n*=19/19; AA, *n*=14/14; BB, *n*=14/14; CC, *n*=16/17; DD, *n*=16/18; EE, *n*=17/18.

Temporal patterning of DV tissues is coordinated with AP patterning modulated by Wnt signaling

To examine whether DV patterning along the AP axis is coordinated with AP patterning by Wnt signaling, we inhibited Wnt signaling in combination with temporally inhibiting BMP signaling. Several chemical Wnt inhibitors that we tested had no effect on early embryos (data not shown); therefore, we used Tg(*hsp70:dkk1GFP*) (Stoick-Cooper et al., 2007) to inhibit Wnt signaling. Because Wnt signaling also functions in DV patterning before and after the mid-blastula stages (reviewed by Langdon and Mullins, 2011), Tg(*hsp70:dkk1GFP*) embryos were subject to HS at 50% epiboly (5.3 hpf) for 1 hour, which we found caused a specific AP patterning defect with minimal DV patterning effects. This HS condition led to the specific expansion of *otx2* expression posteriorly (an anteriorization) without an expansion ventrally (compare Fig. 3B with 3G).

Since the Tg(*hsp70:dkk1*) line was used for inhibiting Wnt signaling, we could not also use the HS-driven Tg(*hsp70:chd*) to temporally inhibit BMP signaling. Therefore, to inhibit BMP signaling we used DMH1, a more selective inhibitor of the type I BMP receptors Alk2 and Alk3 (also known as Acvr1l and Bmpr1aa) than dorsomorphin (Hao et al., 2010). To determine the efficiency with which DMH1 inhibits BMP signaling, we examined P-Smad1/5 levels by western blot analysis at multiple time points after DMH1 treatment, similar to our previous analysis of the effectiveness of Tg(*hsp70:chd*) (Tucker et al., 2008). DMH1 treatment beginning at the 64-cell stage (2 hpf), 1000-cell stage (3 hpf), and high (3.5 hpf) and sphere (4 hpf) stages caused greatly reduced P-Smad1/5 by 40% epiboly (5 hpf), shield (6 hpf), 60% epiboly (6.5 hpf) and 65% epiboly (7 hpf), respectively (Fig. 3A). These results show that DMH1 significantly inhibits P-Smad1/5 levels ~3 hours after treatment is initiated and that DMH1 can be used to temporally inhibit BMP signaling.

The temporal series of DMH1 treatments caused the same dorsalized phenotypes as the Tg(*hsp70:chd*) HS series, except with a 2-hour delay, consistent with the temporal effects of DMH1 treatment on P-Smad1/5 levels (3 hours to inhibit BMP signaling, Fig. 3A) compared with Tg(*hsp70:chd*) [<1 hour to inhibit BMP signaling after HS is initiated (Tucker et al., 2008)]. Treatment of embryos with DMH1 at the 64-cell stage, 1000-cell stage, high and sphere stages phenocopied the dorsalization caused by HS of Tg(*hsp70:chd*) embryos at sphere, 40% epiboly, 50% epiboly (5.3 hpf) and shield stages, respectively (compare Fig. 3C-F with Fig. 2C-F). Thus, DMH1 exhibits a 2-hour delay in its effectiveness compared with Tg(*hsp70:chd*), both in reducing P-Smad1/5 levels and in affecting DV patterning.

We then investigated how the temporal patterning of BMP signaling is affected when the embryo is posteriorized by Wnt signal

inhibition. DMH1 treatment at the 64-cell and 1000-cell stages caused expansion of *otx2* to the ventral side, whereas DMH1 treatment at or after high stage did not alter *otx2* expression (Fig. 3C-F). Inhibition of Wnt signaling by a 1-hour HS at 50% epiboly of Tg(*hsp70:dkk1*) embryos caused *otx2* to expand posteriorly (Fig. 3G). This posteriorly expanded *otx2* expression domain (Fig. 3H-K) was patterned at the same temporal interval as the normally positioned *otx2* domain (Fig. 3C-F).

To activate Wnt signaling and posteriorize the embryos, we treated them with LiCl, which blocks the function of the Wnt inhibitor GSK3 (Klein and Melton, 1996). LiCl treatment caused expression of *hoxb1b*, a marker of caudal hindbrain, to expand anteriorly (Fig. 3Q) (Kudoh et al., 2002). Tg(*hsp70:chd*) embryos that were subject to HS at shield (6 hpf) and 65% epiboly (7 hpf) stages displayed expansion of *hoxb1b* expression fully to the ventral side (Fig. 3M,N), whereas embryos with HS at or after 70% epiboly (7.5 hpf) displayed normal *hoxb1b* expression (Fig. 3O,P). We then investigated whether BMP signaling patterns the rostrally expanded *hoxb1b* tissue at the same time as the normal *hoxb1b* expression domain is patterned or at an earlier time point corresponding to its more rostral location. When we treated Tg(*hsp70:chd*) embryos with LiCl and performed a HS series, we found that the rostrally expanded *hoxb1b* domain was patterned during the same temporal interval as the normally positioned *hoxb1b* domain (Fig. 3, compare M-P and R-U). These data are consistent with the model that DV patterning along the AP axis is coordinated with AP patterning by Wnt signaling.

We examined patterning at a later stage to confirm these results. We analyzed *six3* and *krox20* (*egr2* – Zebrafish Information Network) at the 6-somite stage as markers of anterior neurectoderm and rhombomeres 3 and 5, respectively (Fig. 3V). HS of Tg(*hsp70:chd*) embryos at sphere (4 hpf) and 40% epiboly (5 hpf) stages caused *krox20* expression to expand fully to the ventral side (Fig. 3W,X). HS at 50% epiboly (5.3 hpf) also caused *krox20* rhombomere 5 expression to fully expand, whereas the rhombomere 3 domain was restricted to the dorsal side (Fig. 3Y). HS at shield stage (6 hpf) now resulted in both rhombomeres 5 and 3 being restricted to the dorsal region (Fig. 3Z) (Tucker et al., 2008). Activation of Wnt signaling by LiCl caused *krox20* expression to be shifted anteriorly and a loss of *six3* expression at the 6-somite stage (Fig. 3AA) (Kim et al., 2002; van de Water et al., 2001). This anteriorly shifted posterior tissue (Fig. 3BB-EE) was patterned during the same temporal interval as the normally positioned posterior tissue (Fig. 3W-Z). In conclusion, these results confirm that DV patterning by BMP signaling along the AP axis is coordinated with AP patterning by Wnt signaling.

Temporal patterning of DV tissues is coordinated with AP patterning modulated by RA signaling

To examine whether DV patterning is coordinated with AP patterning mediated by RA signaling, we inhibited RA signaling, a posteriorizing factor. RA signaling was abrogated with 4-(diethylamino)-benzaldehyde (DEAB), a potent retinaldehyde dehydrogenase inhibitor (Russo et al., 1988). We examined expression of *hoxb1a* in rhombomere 4 at the 6-somite stage, which is expanded posteriorly by inhibition of RA (Fig. 4G-L) (Maves and Kimmel, 2005). Inhibition of BMP signaling by HS of Tg(*hsp70:chd*) embryos at sphere (4 hpf), 40% epiboly (5 hpf) and 50% epiboly (5.3 hpf) stages caused *hoxb1a* expression to expand ventrally (Fig. 4B-D). Embryos subject to HS at or after germ ring stage (5.7 hpf) showed normal expression of *hoxb1a* in the dorsal region (Fig. 4E,F). The caudally expanded rhombomere 4 tissue caused by DEAB treatment (Fig. 4H-L) was patterned with the same timing as the normally positioned rhombomere 4 (Fig. 4B-F).

To activate RA signaling and posteriorize the embryos, we treated them with RA. RA treatment caused expression of the caudal hindbrain marker *hoxb1b* to expand dramatically anteriorly (Fig. 4R) (Kudoh et al., 2002). In Tg(*hsp70:chd*) embryos with HS at shield and 65% epiboly (7 hpf) stages, *hoxb1b* expression was expanded fully to the ventral side (Fig. 4N,O), whereas embryos with HS at or after 70% epiboly displayed normal *hoxb1b* expression (Fig. 4P,Q).

We then investigated whether BMP signaling patterns the rostrally expanded *hoxb1b* tissue at the same temporal interval as the

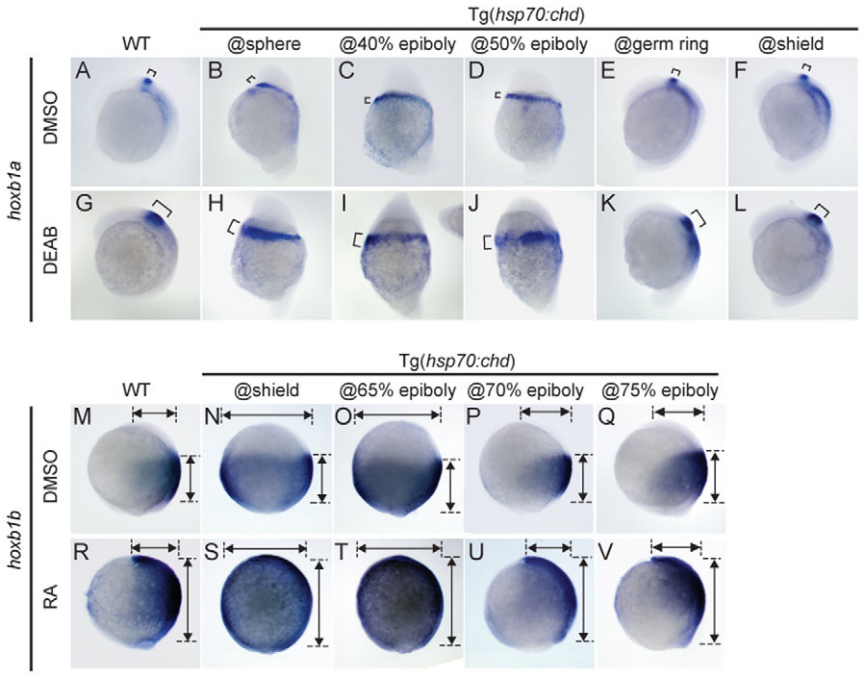

Fig. 4. Posteriorly expanded *hoxb1a* and anteriorly expanded *hoxb1b* caused by altered RA signaling are patterned by BMP signaling with same temporal dynamics as the normal domains. (**A-L**) Expression of *hoxb1a* (bracket) in wild type (A,G) and in Tg(*hsp70:chd*) embryos subject to HS at the indicated stages (B-F,H-L), without (A-F) and with (G-L) DEAB treatment to inhibit RA signaling. (**M-V**) Expression of *hoxb1b* in wild type (M,R) and in Tg(*hsp70:chd*) embryos subject to HS at the indicated stages (N-Q,S-V), without (M-Q) and with (R-V) RA treatment. DEAB and RA treatments began at shield stage. Embryos are shown at (A-L) 6-somite and (M-V) 90% epiboly stages. Lateral views, dorsal to right. A, *n*=19/19; B, *n*=11/11; C, *n*=10/11; D, *n*=9/10; E, *n*=10/12; F, *n*=16/16; G, *n*=19/23; H, *n*=20/24; I, *n*=19/25; J, *n*=25/27; K, *n*=20/23; L, *n*=21/25; M, *n*=14/14; N, *n*=19/22; O, *n*=19/20; P, *n*=22/24; Q, *n*=24/24; R,=20/24; S, *n*=17/20; T, *n*=20/23; U, *n*=21/22; V, *n*=17/20.

normal *hoxb1b* expression domain is patterned or at an earlier time point corresponding to its more rostral location. When we treated Tg(*hsp70:chd*) embryos with RA and performed a series of HSs, we found that the rostrally expanded *hoxb1b* domain was patterned during the same temporal interval as the normally positioned *hoxb1b* region (Fig. 4N-Q,S-V), rather than at an earlier interval corresponding to its new rostral location.

We also examined patterning at a later stage to confirm these results. We analyzed *pax8* expression, a presumptive otic vesicle marker, at the 6-somite stage (Hans and Westerfield, 2007). HS of Tg(*hsp70:chd*) embryos at sphere stage caused a loss of *pax8* expression (supplementary material Fig. S1B). HS at 40% epiboly (5 hpf) caused *pax8* to be expressed in a small anterior ventral region (supplementary material Fig. S1C), whereas HS at 50% epiboly (5.3 hpf) resulted in expression that extended from the dorsal to ventral side (supplementary material Fig. S1D). Finally, HS at shield stage led to the normal dorsal localization of *pax8* (supplementary material Fig. S1E). Activation of RA signaling causes the anterior limit of otic cells to extend rostrally to completely encircle the head (supplementary material Fig. S1F) (Hans et al., 2007; Hans and Westerfield, 2007). This rostrally expanded otic tissue was patterned during the same temporal interval as the normally positioned tissue (supplementary material Fig. S1C-E,H-J). These results indicate that the temporal patterning of DV tissues along the AP axis is coordinated with AP patterning by RA signaling.

Taking all of these results together, we conclude that DV patterning by BMP signaling along the AP axis is coordinated temporally with AP patterning mediated by FGF, Wnt and RA signaling.

P-Smad^{MAPK}, but not P-Smad^{GSK3}, localizes to the ventral vegetal gastrula region

A study in *Xenopus* showed that in dorsal tissues the linker region of Smad1 is sequentially phosphorylated by MAPK and GSK3, causing it to be degraded (Fuentealba et al., 2007). The degradation of P-Smad1 and loss of BMP signaling dorsally then allows neural tissue development and AP patterning by FGF and Wnt signaling. In zebrafish, the ventral P-Smad1/5 gradient appears to be stable along the AP axis until 75% epiboly, when prospective caudal hindbrain tissue is patterned (Fig. 5M-O) (Tucker et al., 2008). These data suggest that a degradation mechanism in ventral vegetal regions does not regulate the temporal function of BMP signaling in zebrafish. We tested whether a modified mechanism might be acting in which P-Smad1/5 function is inhibited by FGF/MAPK and Wnt/GSK3 through a non-degradation mechanism to temporally coordinate DV and AP patterning during gastrulation. We investigated the localization of GSK3-phosphorylated Smad1/5 (P-Smad1/5^{GSK3}) and MAPK-phosphorylated Smad1/5 (P-Smad1/5^{MAPK}) using antibodies specific for the phosphorylated forms of human SMAD1 (Fuentealba et al., 2007).

We tested the specificity of the human P-Smad1^{MAPK} and P-Smad1^{GSK3} antibodies for zebrafish Smad5 and for their respective phosphorylation sites. The *smad5* gene in zebrafish is expressed maternally and functions predominantly over *smad1* for specification of ventral fates (Dick et al., 1999; Hild et al., 1999; Kramer et al., 2002). In the zebrafish Smad5 protein, the equivalent human MAPK and GSK3 phosphorylation sites in the SMAD1 linker region are present (supplementary material Fig. S2). In the zebrafish *smad5* mutant *somitabun*^{dtc24} (*sbn*^{dtc24}), we found that P-Smad1/5^{MAPK} and P-Smad1/5^{GSK3} signals were greatly reduced or absent, similar to the BMP receptor phosphorylated form of Smad1/5, P-Smad1/5 (Fig. 5A,E,I). When we injected human *SMAD1* RNA (*hSmad1WT*) into *sbn*^{dtc24} zebrafish embryos, the P-Smad1^{MAPK} and P-Smad1^{GSK3} signals were rescued and localized to ventral regions (Fig. 5B,F,J). Moreover, when we injected *sbn*^{dtc24} mutant embryos with human *SMAD1* mRNA that had mutations in the MAPK (*hSmad1MM*) or the GSK3 (*hSmad1GM*) phosphorylation sites (Fuentealba et al., 2007), we detected no P-Smad1^{MAPK} or P-Smad1^{GSK3} immunostaining, respectively (Fig. 5G,K). From these results, we conclude that P-Smad1^{MAPK} and P-Smad1^{GSK3} antibodies specifically detect their respective

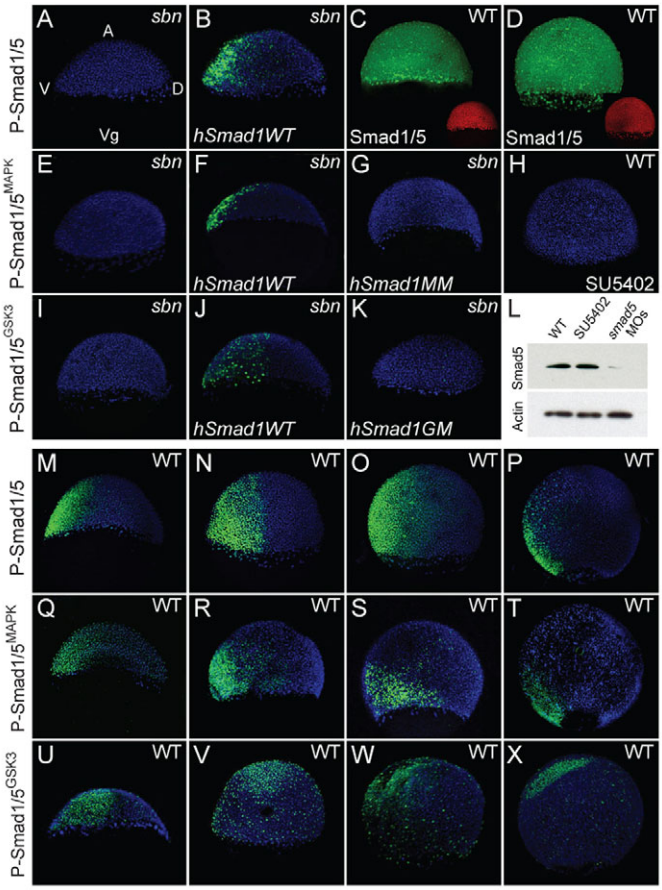

Fig. 5. Localization of P-Smad1/5^{MAPK}, P-Smad1/5^{GSK3} and total Smad1/5 during gastrulation. (**A-K**) Localization of P-Smad1/5 (A, *n*=4/4; B, *n*=5/6), total Smad1/5 (C, *n*=6/6; D, *n*=5/5), P-Smad1/5^{MAPK} (E, *n*=5/5; F, *n*=4/5; G, *n*=3/3; H, *n*=7/7) and P-Smad1/5^{GSK3} (I, *n*=3/3; J, *n*=4/4; K, *n*=2/3) in *sbn*^{dtc24} mutants (A,B,E-G,I-K) or wild type (C,D,H) at early gastrula stage (A-C,E-G,I-K), 75% epiboly (D) or 60% epiboly (H) stage. Embryos were injected with *hSmad1WT* (B,F,J), *hSmad1MM* (G) or *hSmad1GM* (K) RNA or were treated with SU5402 (H). (**L**) Western blot of total Smad5 protein in wild-type embryos and those treated with SU5402 or injected with *smad5* MOs. Embryos were collected at 65% epiboly. Actin is a loading control. (**M-X**) Localization of P-Smad1/5 (M-P), P-Smad1/5^{MAPK} (Q-T) and P-Smad1/5^{GSK3} (U-X) in wild type at shield (early gastrula) (M, *n*=8/8; Q, *n*=10/12; U, *n*=9/10), 70% epiboly (N, *n*=6/6; R, *n*=9/13; V, *n*=3/5), 80% epiboly (O, *n*=7/7; S, *n*=12/15; W, *n*=4/5) and 90% epiboly (late gastrula) (P, *n*=7/7; T, *n*=8/11; X, *n*=3/5) stage. All are merged confocal images of P-Smad1/5 (green), total Smad1/5 (green), P-Smad1/5^{MAPK} (green), P-Smad1/5^{GSK3} (green) and DAPI (blue, except red in for C,D). Lateral views, dorsal to right. A, animal pole; Vg, vegetal pole; V, ventral; D, dorsal.

phosphorylation sites in the zebrafish Smad5 linker region. Furthermore, wild-type embryos treated with the FGF inhibitor SU5402 lacked P-Smad1/5^{MAPK}, indicating that P-Smad1/5^{MAPK} is specific for FGF signaling (compare Fig. 5H with 5R).

Although FGF and Wnt signaling are also present in dorsal marginal gastrula regions, we did not detect P-Smad1/5^{MAPK} or P-Smad1/5^{GSK3} dorsally. To determine if Smad1/5 protein is present dorsally, we examined total Smad1/5 protein localization by whole-mount immunostaining. We found that Smad1/5 protein is present uniformly in both dorsal and ventral gastrula regions of the zebrafish embryo (Fig. 5C,D) and is absent from embryos injected with *smad5* MOs (data not shown). Moreover, inhibition of FGF signaling did not change the total Smad1/5 level as determined by western blot analysis, indicating that FGF signaling does not affect the overall Smad5 level (Fig. 5L). These results are consistent with the previously reported requirement for BMP receptor phosphorylation of Smad1/5 prior to phosphorylation by MAPK or GSK3 (Fuentealba et al., 2007).

We then examined the localization of P-Smad1/5^{MAPK} and P-Smad1/5^{GSK3} during gastrulation. P-Smad1/5^{MAPK} localized to ventral regions of the early gastrula, with high signal in the marginal region and lower levels animally (Fig. 5Q). P-Smad1/5^{MAPK} was maintained in a ventral vegetal region as gastrulation and epiboly progressed (Fig. 5R-T). By contrast, P-Smad1/5^{GSK3} localized strongly to the entire ventral region of the early gastrula (Fig. 5U) and then shifted to an animal region during gastrulation (Fig. 5V-X). Because vegetal regions correspond to more posterior regions of the early embryo, these results suggest that FGF/MAPK, but not GSK3, phosphorylation of Smad5 is positioned in a region where it could temporally regulate BMP signaling along the AP axis.

FGF/MAPK Smad5 linker phosphorylation affects temporal patterning of DV tissues

To test whether the temporal patterning of DV tissues along the AP axis is modulated by the FGF/MAPK phosphorylation of the Smad1/5 linker, we examined the effect of mutating these phosphorylation sites. We depleted Tg(*hsp70:chd*) embryos of endogenous Smad5 by injecting *smad5* MOs. We then injected these embryos with *hSmad1WT* RNA as a control or *hSmad1MM* mRNA, which has the serine/threonine phosphorylation sites mutated to alanine (Fuentealba et al., 2007). Injection of three doses of RNA into *smad5*-depleted embryos revealed that the *hSmad1WT* and *hSmad1MM* mRNAs have similar rescuing activity (supplementary material Fig. S3A). In addition, the Smad1 protein level in *hSmad1WT*- and *hSmad1MAPK*-injected embryos was similar based on western blot analysis (supplementary material Fig. S3B, noHS), suggesting that the hSmad1WT and hSmad1MM proteins have similar stability in the injected embryos. We then performed a series of HSs to investigate the temporal patterning of BMP signaling using Tg(*hsp70:chd*).

We investigated the temporal function of *hSmad1MM* in specifying DV tissues by analyzing the expression domain of *hoxb1b*, a prospective caudal hindbrain marker. We analyzed the strength of dorsalization by measuring the DV extent of *hoxb1b* expression relative to the overall DV embryo width. We classified the embryos as: 'fully dorsalized' if *hoxb1b* was expanded to 100% of the embryo width; 'weakly dorsalized' if expression was 66-99% of embryo width; 'wild-type' if expression was 50-66% of embryo width; and 'ventralized' for an expression domain that was less than 50% of the embryo width. Depletion of Smad5 by injection of *smad5* MOs into Tg(*hsp70:chd*) embryos caused *hoxb1b* expression to expand fully around the ventral side independently of the HS treatments (Fig. 6B,E, second bar in each set). Injection of *hSmad1WT* or *hSmad1MM* mRNA into these embryos rescued *hoxb1b* expression to its normal expression domain (Fig. 6E, third and fourth bars of first set). Following a series of HSs of Tg(*hsp70:chd*), *hSmad1WT*-injected embryos showed the same temporal patterning of *hoxb1b* as wild-type embryos, with normal dorsally restricted *hoxb1b* expression by HS at and after the 70% epiboly stage (Fig. 6E, third bar in sets two to five; compare with Fig. 4N-Q). By contrast, injection of *hSmad1MM* mRNA caused 30-minute earlier specification of *hoxb1b*, as evident with HS at the 65% epiboly stage, compared with *hSmad1WT*-injected embryos (Fig. 6A-E). Injection of three different doses (250, 350 and 450 pg) of *hSmad1WT* and *hSmad1MM* also showed that only *hSmad1MM* leads to precocious patterning of the posterior ventral tissue, independent of the mRNA dose injected (supplementary material Fig. S4).

We similarly monitored dorsalization of anterior regions by examining expression of *otx2*. In addition, we examined *no tail* (*ntl*) expression in the notochord to allow us to precisely orient the embryos and determine the extent of dorsalization. We measured the DV width of the *otx2* expression domain and compared it with the overall DV width of the embryo. The *otx2* domain in wild-type embryos varied from 46 to 53% (n=8) of embryo width. In fully dorsalized embryos, the *otx2* domain was 83-89% of embryo width (n=9; it is not 100% because the overall DV embryo width is measured at its widest point and the *otx2* domain lies more anteriorly, where the DV width is narrower). We established four classes of phenotype: 'fully dorsalized', corresponding to an *otx2* domain of 83-89% embryo width; 'weakly dorsalized', corresponding to 54-82% of embryo width; 'wild-type', corresponding to 46-53% of embryo width; and 'ventralized', corresponding to less than 46% embryo width.

Depletion of Smad5 by injection of *smad5* MOs into Tg(*hsp70:chd*) embryos caused *otx2* expression to expand fully to the ventral side independently of HS (Fig. 6G,J, second bar in each set). Injection of *hSmad1WT* or *hSmad1MM* mRNA into these embryos rescued *otx2* expression to its normal domain (Fig. 6J, third and fourth bar in first set, respectively). Following a series of HSs of Tg(*hsp70:chd*) embryos, we found that *hSmad1WT* mRNA rescued *otx2* expression to its normal dorsal region when subject to HS at and after the 50% epiboly stage, as observed in wild-type embryos (Fig. 6J, compare first and third bar in sets two to five; see also Fig. 1G-L). By contrast, injection of *hSmad1MM* caused 30-minute earlier specification of the *otx2* domain, as evident with HS at the 40% epiboly stage, compared with *hSmad1WT*-injected embryos (Fig. 6H-J, compare the third and fourth bars in set three). These results suggest that FGF signaling through MAPK phosphorylates the linker of P-Smad1/5 in ventral vegetal regions of the embryo, inhibiting P-Smad1/5 activity. Thus, FGF/MAPK signaling in part controls the temporal patterning of DV tissues along the AP axis.

DISCUSSION

Here we show that there is an intimate coordination in the temporal patterning of DV tissues with AP patterning during zebrafish gastrulation. Altering AP patterning by activation or inhibition of FGF, Wnt or RA signaling pathways, in combination with temporal BMP inhibition, revealed that DV patterning by BMP signaling along the AP axis is coordinated with AP patterning (Fig. 7). A gradual shift of P-Smad1/5^{MAPK} in ventral vegetal regions during gastrulation suggests that FGF/MAPK could regulate the temporal patterning of BMP signaling along the AP axis (Fig. 7). We also

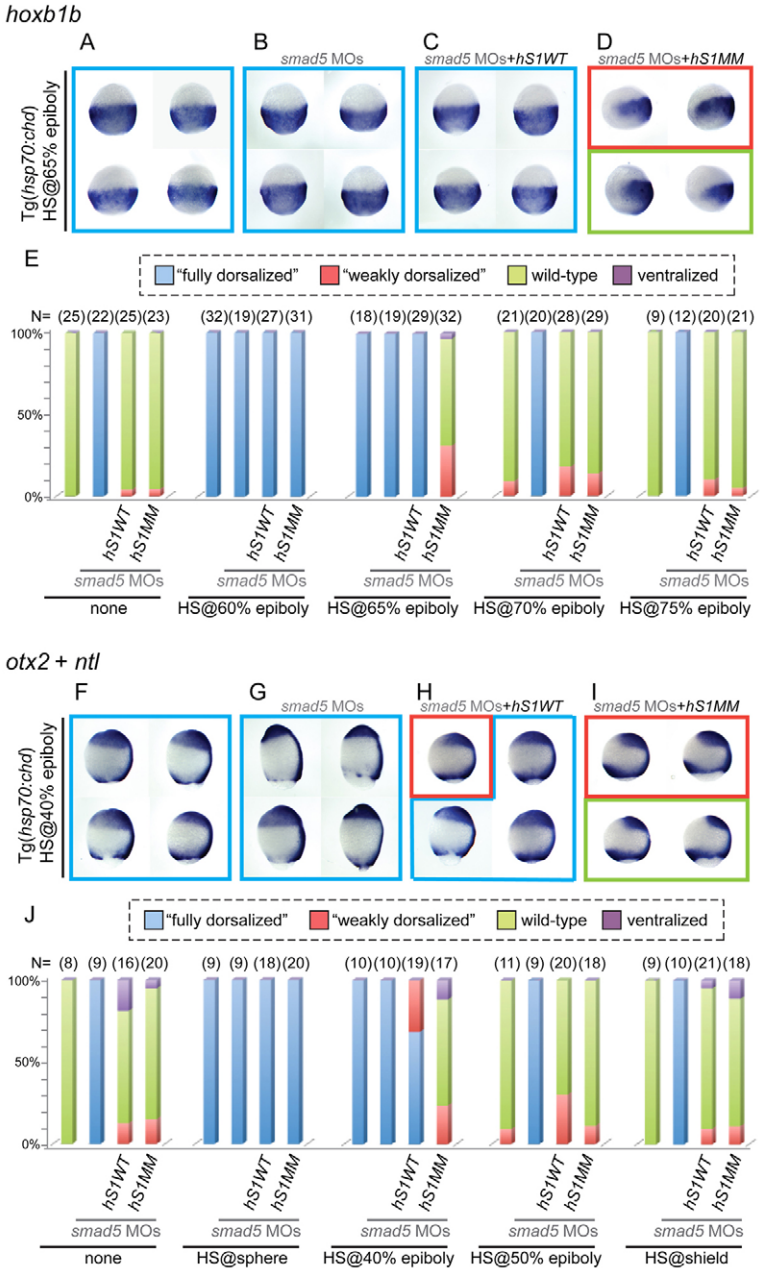

Fig. 6. FGF/MAPK affects temporal patterning of DV tissues through the P-Smad5 linker region. (**A-D**) *hoxb1b* expression in Tg(*hsp70:chd*) embryos with HS at 65% epiboly. Lateral views, dorsal to right at 90-100% epiboly stage. Embryos were injected with *smad5* MOs (B), *smad5* MOs and *hSmad1WT* (*hS1WT*) mRNA (C) or *smad5* MOs and *hSmad1* MAPK mutant (*hS1MM*) mRNA (D). (**E**) The percentage of embryos exhibiting a fully dorsalized, weakly dorsalized, wild-type or ventralized phenotype in the various conditions. (**F-I**) *otx2* and *ntl* expression in Tg(*hsp70:chd*) embryos with HS at 40% epiboly. Lateral views, dorsal to right at 80% epiboly. Embryos were injected with *smad5* MOs (G), *smad5* MOs and *hS1WT* mRNA (H) or *smad5* MOs and *hS1MM* mRNA (I). (**J**) The percentage of embryos exhibiting the different dorsalization strength phenotypes in the various conditions. The panel borders in A-D and F-I match the phenotype colors in E and J.

showed that the temporal coordination of DV and AP patterning is in part mediated by FGF/MAPK (Fig. 6). Replacing Smad5 with hSmad1MM, which lacks the MAPK linker phosphorylation sites, caused precocious patterning of DV tissues. DV tissues in both anterior and posterior regions were patterned 30 minutes earlier by hSmad1MM. These results suggest that MAPK phosphorylation of the P-Smad1/5 linker normally inhibits BMP signaling by ~30 minutes in both anterior and posterior regions. Although tissues are patterned precociously when Smad1/5 lacks the MAPK phosphorylation sites, the progressive patterning of DV tissues continues, suggesting that additional factors also regulate the temporal coordination of DV and AP patterning.

In addition to FGF/MAPK, a Wnt signaling component could be involved in coordinating DV and AP patterning. Our data indicate that DV patterning along the AP axis is coordinated with AP patterning by Wnt signaling. However, in contrast to P-Smad1/5^{MAPK}, P-Smad1/5^{GSK3} was shifted to animal regions during gastrulation, suggesting that FGF/MAPK works independently of GSK3 to temporally regulate DV patterning through phosphorylation of the Smad1/5 linker region. However, the data do not exclude the possibility that the temporal coordination of DV and AP patterning is also mediated by Wnt signaling. It is possible that a Wnt signaling component other than GSK3 modulates DV temporal patterning along the AP axis. Further studies are needed to elucidate which component of the Wnt signaling pathway might temporally modulate BMP signaling during DV patterning.

In addition to the FGF and Wnt signaling components, RA signaling components could also be involved in coordinating DV and AP patterning. Nuclear RA receptor γ (RARγ) agonists decrease phosphorylation of Smad1/5/8 in mouse chondrocytic ADTC5 cells (Shimono et al., 2011). In mouse P19 (teratocarcinoma) cells and in the chick neural tube, RA promotes the degradation of P-Smad1 through MAPK activation (Sheng et al., 2010). Because P-Smad1/5

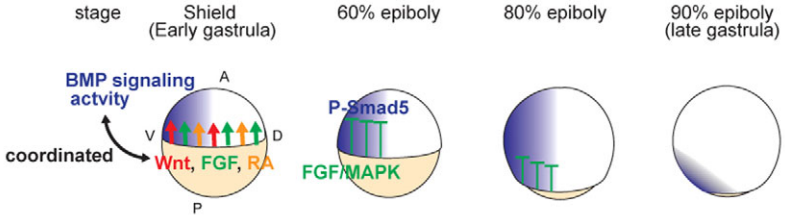

Fig. 7. Model of coordinated patterning of DV and AP tissues. DV patterning by BMP signaling along the AP axis and temporally progressive AP patterning by Wnt, FGF and RA signaling are coordinated during gastrulation. FGF/MAPK inhibits P-Smad5 through phosphorylation of its linker region and thereby DV and AP tissues are temporally patterned progressively. As FGF/MAPK signaling within the margin moves vegetally (posteriorly) during epiboly progression, its inhibition of P-Smad1/5 becomes localized to progressively more posterior regions. Although Wnt and RA signaling remain within the margin during gastrulation, it is not known whether these signals act directly in temporally regulating BMP signaling in DV patterning. A, anterior; V, ventral; D, dorsal; P, posterior.

appears stable along the AP axis during zebrafish gastrulation (Fig. 5) (Tucker et al., 2008), another mechanism is expected to operate to coordinate patterning.

Based on our results, we propose that MAPK phosphorylation of the P-Smad1/5 linker reduces P-Smad1/5 function and thus acts in part to temporally regulate BMP signaling along the AP axis (Fig. 7). In *Xenopus*, the combined phosphorylation of the Smad1 linker by MAPK and GSK3 in dorsal tissues causes P-Smad1 degradation, thus blocking BMP signaling dorsally and allowing AP neural patterning (Fuentealba et al., 2007). In zebrafish, degradation of Smad5 is not evident in the marginal zone where FGF/MAPK activity exists and Smad5 levels appear unaffected when FGF signaling is inhibited (Fig. 5). Furthermore, in ventral tissues the P-Smad5 gradient appears stable along the AP axis and thus degradation of P-Smad1/5 is unlikely to regulate its temporal function along the AP axis during gastrulation (Fig. 5) (Tucker et al., 2008). We propose that, in ventral vegetal gastrula regions, FGF/MAPK in the absence of GSK3 negatively regulates P-Smad1/5 function in a distinct manner, possibly affecting its activity directly.

In *Xenopus* and zebrafish, AP tissues are temporally patterned progressively from anterior to posterior, as is evident in the earlier developmental expression of anterior compared with more posterior neurectodermal markers (Gamse and Sive, 2000; Gamse and Sive, 2001; Kudoh et al., 2002; Maves and Kimmel, 2005). The timing of specification also indicates temporally progressive AP patterning. Forebrain tissue is specified in the early gastrula (Grinblat et al., 1998), whereas the hindbrain is specified in mid-gastrula (Woo and Fraser, 1998). Here we showed that neurectodermal tissues are temporally patterned progressively from prospective forebrain to caudal hindbrain during late blastula to mid- to late gastrula stages (Fig. 1) (Tucker et al., 2008). Thus, AP and DV patterning are temporally coordinated, allowing cells to adopt both an AP and a DV identity simultaneously from anterior to posterior during blastula and gastrula stages.

Possible involvement of other factors in the coordinated patterning of DV and AP tissues

Nodal is expressed in the marginal zone of the zebrafish gastrula (Erter et al., 1998; Rebagliati et al., 1998a; Rebagliati et al., 1998b; Sampath et al., 1998) and can posteriorize tissues dose dependently. Injection of *antivin* (*lefty1* – Zebrafish Information Network) mRNA, which inhibits Nodal signaling activity, into zebrafish embryos causes a dose-dependent truncation of posterior tissues (Thisse et al., 2000). A genetic study in zebrafish has suggested that AP patterning by Nodal signaling is indirect, acting in part by regulating *wnt8* expression (Erter et al., 2001).

In *Xenopus*, the transcription factor *foxb1* was recently reported to coordinate DV and AP patterning of the ectoderm (Takebayashi-Suzuki et al., 2011). *foxb1* is expressed in the posterior dorsal ectoderm of the *Xenopus* (Gamse and Sive, 2001) and zebrafish (Grinblat et al., 1998) gastrula and, when overexpressed in *Xenopus*, can negatively regulate BMP signaling (Takebayashi-Suzuki et al., 2011). Depletion of Foxb1 showed that it functions in AP patterning; however, a function in DV patterning was not found (Takebayashi-Suzuki et al., 2011). Thus, *foxb1* regulates AP patterning but is unlikely to directly coordinate DV and AP patterning.

Epiboly movements and the coordinated patterning of DV and AP tissues

During gastrulation, the vertebrate body plan is established by evolutionarily conserved cell movements, such as epiboly and convergence and extension (C&E) movements (reviewed by Leptin, 2005; Montero and Heisenberg, 2004; Solnica-Krezel, 2005; Yin et al., 2009). Considering that BMP signaling regulates C&E movements of lateral mesodermal cells independently of DV patterning (von der Hardt et al., 2007) and that cranial DV tissues are patterned prior to the major C&E movements (Fig. 1) (Tucker et al., 2008), C&E cell movements are not expected to be related to the coordinated patterning of DV and AP tissues. However, we believe that epiboly movements play a key role in regulating the temporal patterning of DV tissues by moving the domain of FGF/MAPK signaling posteriorly during gastrulation. As epiboly proceeds during gastrulation, FGF/MAPK phosphorylation of the P-Smad1/5 linker becomes localized to progressively more posterior (vegetal) regions, allowing tissues to be temporally patterned and specified progressively in its wake (Fig. 7). Thus, this cell movement mechanism allows both AP and DV tissues to be temporally patterned progressively in a coordinate manner.

Acknowledgements
We thank Drs E. De Robertis and L. C. Fuentealba for the hSmad1WT and hSmad1MM constructs and P-Smad1/5^{MAPK} and P-Smad1/5^{GSK3} antibodies; C. Hong for DMH1; M. Hibi and S. Maegawa for SU5402; R. T. Moon for Tg(*hsp70:dkk1GFP*); V. Prince for the *hoxb1a* plasmid; and J. Dutko, Y. Elkouby and Y. Langdon for comments on this manuscript.

Funding
This work was supported by the National Institutes of Health [NIH R01GM56326 to M.C.M.]. Deposited in PMC for release after 12 months.

Competing interests statement
The authors declare no competing financial interests.

Supplementary material
Supplementary material available online at
http://dev.biologists.org/lookup/suppl/doi:10.1242/dev.088104/-/DC1

References

Alexandre, D., Clarke, J. D., Oxtoby, E., Yan, Y. L., Jowett, T. and Holder, N. (1996). Ectopic expression of Hoxa-1 in the zebrafish alters the fate of the mandibular arch neural crest and phenocopies a retinoic acid-induced phenotype. *Development* **122**, 735-746.

Dick, A., Meier, A. and Hammerschmidt, M. (1999). Smad1 and Smad5 have distinct roles during dorsoventral patterning of the zebrafish embryo. *Dev. Dyn.* **216**, 285-298.

Erter, C. E., Solnica-Krezel, L. and Wright, C. V. (1998). Zebrafish nodal-related 2 encodes an early mesendodermal inducer signaling from the extraembryonic yolk syncytial layer. *Dev. Biol.* **204**, 361-372.

Erter, C. E., Wilm, T. P., Basler, N., Wright, C. V. and Solnica-Krezel, L. (2001). Wnt8 is required in lateral mesendodermal precursors for neural posteriorization in vivo. *Development* **128**, 3571-3583.

Fuentealba, L. C., Eivers, E., Ikeda, A., Hurtado, C., Kuroda, H., Pera, E. M. and De Robertis, E. M. (2007). Integrating patterning signals: Wnt/GSK3 regulates the duration of the BMP/Smad1 signal. *Cell* **131**, 980-993.

Fürthauer, M., Van Celst, J., Thisse, C. and Thisse, B. (2004). Fgf signalling controls the dorsoventral patterning of the zebrafish embryo. *Development* **131**, 2853-2864.

Gamse, J. and Sive, H. (2000). Vertebrate anteroposterior patterning: the Xenopus neurectoderm as a paradigm. *BioEssays* **22**, 976-986.

Gamse, J. T. and Sive, H. (2001). Early anteroposterior division of the presumptive neurectoderm in Xenopus. *Mech. Dev.* **104**, 21-36.

Grinblat, Y., Gamse, J., Patel, M. and Sive, H. (1998). Determination of the zebrafish forebrain: induction and patterning. *Development* **125**, 4403-4416.

Hans, S. and Westerfield, M. (2007). Changes in retinoic acid signaling alter otic patterning. *Development* **134**, 2449-2458.

Hans, S., Christison, J., Liu, D. and Westerfield, M. (2007). Fgf-dependent otic induction requires competence provided by Foxi1 and Dlx3b. *BMC Dev. Biol.* **7**, 5.

Hao, J., Ho, J. N., Lewis, J. A., Karim, K. A., Daniels, R. N., Gentry, P. R., Hopkins, C. R., Lindsley, C. W. and Hong, C. C. (2010). In vivo structure-activity relationship study of dorsomorphin analogues identifies selective VEGF and BMP inhibitors. *ACS Chem. Biol.* **5**, 245-253.

Hild, M., Dick, A., Rauch, G. J., Meier, A., Bouwmeester, T., Haffter, P. and Hammerschmidt, M. (1999). The smad5 mutation somitabun blocks Bmp2b signaling during early dorsoventral patterning of the zebrafish embryo. *Development* **126**, 2149-2159.

Houart, C., Caneparo, L., Heisenberg, C., Barth, K., Take-Uchi, M. and Wilson, S. (2002). Establishment of the telencephalon during gastrulation by local antagonism of Wnt signaling. *Neuron* **35**, 255-265.

Kim, S. H., Shin, J., Park, H. C., Yeo, S. Y., Hong, S. K., Han, S., Rhee, M., Kim, C. H., Chitnis, A. B. and Huh, T. L. (2002). Specification of an anterior neuroectoderm patterning by Frizzled8a-mediated Wnt8b signalling during late gastrulation in zebrafish. *Development* **129**, 4443-4455.

Klein, P. S. and Melton, D. A. (1996). A molecular mechanism for the effect of lithium on development. *Proc. Natl. Acad. Sci. USA* **93**, 8455-8459.

Kobayashi, M., Toyama, R., Takeda, H., Dawid, I. B. and Kawakami, K. (1998). Overexpression of the forebrain-specific homeobox gene six3 induces rostral forebrain enlargement in zebrafish. *Development* **125**, 2973-2982.

Kramer, C., Mayr, T., Nowak, M., Schumacher, J., Runke, G., Bauer, H., Wagner, D. S., Schmid, B., Imai, Y., Talbot, W. S. et al. (2002). Maternally supplied Smad5 is required for ventral specification in zebrafish embryos prior to zygotic Bmp signaling. *Dev. Biol.* **250**, 263-279.

Krauss, S., Maden, M., Holder, N. and Wilson, S. W. (1992). Zebrafish pax[b] is involved in the formation of the midbrain-hindbrain boundary. *Nature* **360**, 87-89.

Kudoh, T., Wilson, S. W. and Dawid, I. B. (2002). Distinct roles for Fgf, Wnt and retinoic acid in posteriorizing the neural ectoderm. *Development* **129**, 4335-4346.

Kudoh, T., Concha, M. L., Houart, C., Dawid, I. B. and Wilson, S. W. (2004). Combinatorial Fgf and Bmp signalling patterns the gastrula ectoderm into prospective neural and epidermal domains. *Development* **131**, 3581-3592.

Langdon, Y. G. and Mullins, M. C. (2011). Maternal and zygotic control of zebrafish dorsoventral axial patterning. *Annu. Rev. Genet.* **45**, 357-377.

Leptin, M. (2005). Gastrulation movements: the logic and the nuts and bolts. *Dev. Cell* **8**, 305-320.

Li, Y., Allende, M. L., Finkelstein, R. and Weinberg, E. S. (1994). Expression of two zebrafish orthodenticle-related genes in the embryonic brain. *Mech. Dev.* **48**, 229-244.

Little, S. C. and Mullins, M. C. (2006). Extracellular modulation of BMP activity in patterning the dorsoventral axis. *Birth Defects Res. C Embryo Today* **78**, 224-242.

Maden, M. (2002). Retinoid signalling in the development of the central nervous system. *Nat. Rev. Neurosci.* **3**, 843-853.

Maegawa, S., Varga, M. and Weinberg, E. S. (2006). FGF signaling is required for beta-catenin-mediated induction of the zebrafish organizer. *Development* **133**, 3265-3276.

Maves, L. and Kimmel, C. B. (2005). Dynamic and sequential patterning of the zebrafish posterior hindbrain by retinoic acid. *Dev. Biol.* **285**, 593-605.

Mohammadi, M., McMahon, G., Sun, L., Tang, C., Hirth, P., Yeh, B. K., Hubbard, S. R. and Schlessinger, J. (1997). Structures of the tyrosine kinase domain of fibroblast growth factor receptor in complex with inhibitors. *Science* **276**, 955-960.

Montero, J. A. and Heisenberg, C. P. (2004). Gastrulation dynamics: cells move into focus. *Trends Cell Biol.* **14**, 620-627.

Mori, H., Miyazaki, Y., Morita, T., Nitta, H. and Mishina, M. (1994). Different spatio-temporal expressions of three otx homeoprotein transcripts during zebrafish embryogenesis. *Brain Res. Mol. Brain Res.* **27**, 221-231.

Mullins, M. C., Hammerschmidt, M., Kane, D. A., Odenthal, J., Brand, M., van Eeden, F. J., Furutani-Seiki, M., Granato, M., Haffter, P., Heisenberg, C. P. et al. (1996). Genes establishing dorsoventral pattern formation in the zebrafish embryo: the ventral specifying genes. *Development* **123**, 81-93.

Nguyen, V. H., Trout, J., Connors, S. A., Andermann, P., Weinberg, E. and Mullins, M. C. (2000). Dorsal and intermediate neuronal cell types of the spinal cord are established by a BMP signaling pathway. *Development* **127**, 1209-1220.

Oxtoby, E. and Jowett, T. (1993). Cloning of the zebrafish krox-20 gene (krx-20) and its expression during hindbrain development. *Nucleic Acids Res.* **21**, 1087-1095.

Prince, V. E., Moens, C. B., Kimmel, C. B. and Ho, R. K. (1998). Zebrafish hox genes: expression in the hindbrain region of wild-type and mutants of the segmentation gene, valentino. *Development* **125**, 393-406.

Ramel, M. C., Buckles, G. R., Baker, K. D. and Lekven, A. C. (2005). WNT8 and BMP2B co-regulate non-axial mesoderm patterning during zebrafish gastrulation. *Dev. Biol.* **287**, 237-248.

Rebagliati, M. R., Toyama, R., Fricke, C., Haffter, P. and Dawid, I. B. (1998a). Zebrafish nodal-related genes are implicated in axial patterning and establishing left-right asymmetry. *Dev. Biol.* **199**, 261-272.

Rebagliati, M. R., Toyama, R., Haffter, P. and Dawid, I. B. (1998b). cyclops encodes a nodal-related factor involved in midline signaling. *Proc. Natl. Acad. Sci. USA* **95**, 9932-9937.

Rhinn, M., Lun, K., Amores, A., Yan, Y. L., Postlethwait, J. H. and Brand, M. (2003). Cloning, expression and relationship of zebrafish gbx1 and gbx2 genes to Fgf signaling. *Mech. Dev.* **120**, 919-936.

Rhinn, M., Lun, K., Luz, M., Werner, M. and Brand, M. (2005). Positioning of the midbrain-hindbrain boundary organizer through global posteriorization of the neuroectoderm mediated by Wnt8 signaling. *Development* **132**, 1261-1272.

Russo, J. E., Hauguitz, D. and Hilton, J. (1988). Inhibition of mouse cytosolic aldehyde dehydrogenase by 4-(diethylamino)benzaldehyde. *Biochem. Pharmacol.* **37**, 1639-1642.

Sampath, K., Rubinstein, A. L., Cheng, A. M., Liang, J. O., Fekany, K., Solnica-Krezel, L., Korzh, V., Halpern, M. E. and Wright, C. V. (1998). Induction of the zebrafish ventral brain and floorplate requires cyclops/nodal signalling. *Nature* **395**, 185-189.

Schier, A. F. and Talbot, W. S. (2005). Molecular genetics of axis formation in zebrafish. *Annu. Rev. Genet.* **39**, 561-613.

Schulte-Merker, S., Ho, R. K., Herrmann, B. G. and Nüsslein-Volhard, C. (1992). The protein product of the zebrafish homologue of the mouse T gene is expressed in nuclei of the germ ring and the notochord of the early embryo. *Development* **116**, 1021-1032.

Schumacher, J. A., Hashiguchi, M., Nguyen, V. H. and Mullins, M. C. (2011). An intermediate level of BMP signaling directly specifies cranial neural crest progenitor cells in zebrafish. *PLoS ONE* **6**, e27403.

Sheng, N., Xie, Z., Wang, C., Bai, G., Zhang, K., Zhu, Q., Song, J., Guillemot, F., Chen, Y. G., Lin, A. et al. (2010). Retinoic acid regulates bone morphogenic protein signal duration by promoting the degradation of phosphorylated Smad1. *Proc. Natl. Acad. Sci. USA* **107**, 18886-18891.

Shimizu, T., Bae, Y. K., Muraoka, O. and Hibi, M. (2005). Interaction of Wnt and caudal-related genes in zebrafish posterior body formation. *Dev. Biol.* **279**, 125-141.

Shimono, K., Tung, W. E., Macolino, C., Chi, A. H., Didizian, J. H., Mundy, C., Chandraratna, R. A., Mishina, Y., Enomoto-Iwamoto, M., Pacifici, M. et al. (2011). Potent inhibition of heterotopic ossification by nuclear retinoic acid receptor-γ agonists. *Nat. Med.* **17**, 454-460.

Solnica-Krezel, L. (2005). Conserved patterns of cell movements during vertebrate gastrulation. *Curr. Biol.* **15**, R213-R228.

Stern, C. D., Charité, J., Deschamps, J., Duboule, D., Durston, A. J., Kmita, M., Nicolas, J. F., Palmeirim, I., Smith, J. C. and Wolpert, L. (2006). Head-tail patterning of the vertebrate embryo: one, two or many unresolved problems? *Int. J. Dev. Biol.* **50**, 3-15.

Stoick-Cooper, C. L., Weidinger, G., Riehle, K. J., Hubbert, C., Major, M. B., Fausto, N. and Moon, R. T. (2007). Distinct Wnt signaling pathways have opposing roles in appendage regeneration. *Development* **134**, 479-489.

Takebayashi-Suzuki, K., Kitayama, A., Terasaka-Iioka, C., Ueno, N. and Suzuki, A. (2011). The forkhead transcription factor FoxB1 regulates the dorsal-ventral and anterior-posterior patterning of the ectoderm during early Xenopus embryogenesis. *Dev. Biol.* **360**, 11-29.

Thisse, B., Wright, C. V. and Thisse, C. (2000). Activin- and Nodal-related factors control antero-posterior patterning of the zebrafish embryo. *Nature* **403**, 425-428.
Tucker, J. A., Mintzer, K. A. and Mullins, M. C. (2008). The BMP signaling gradient patterns dorsoventral tissues in a temporally progressive manner along the anteroposterior axis. *Dev. Cell* **14**, 108-119.
van de Water, S., van de Wetering, M., Joore, J., Esseling, J., Bink, R., Clevers, H. and Zivkovic, D. (2001). Ectopic Wnt signal determines the eyeless phenotype of zebrafish masterblind mutant. *Development* **128**, 3877-3888.
von der Hardt, S., Bakkers, J., Inbal, A., Carvalho, L., Solnica-Krezel, L., Heisenberg, C. P. and Hammerschmidt, M. (2007). The Bmp gradient of the zebrafish gastrula guides migrating lateral cells by regulating cell-cell adhesion. *Curr. Biol.* **17**, 475-487.
Wilson, S. W. and Houart, C. (2004). Early steps in the development of the forebrain. *Dev. Cell* **6**, 167-181.
Woo, K. and Fraser, S. E. (1998). Specification of the hindbrain fate in the zebrafish. *Dev. Biol.* **197**, 283-296.
Yin, C., Ciruna, B. and Solnica-Krezel, L. (2009). Convergence and extension movements during vertebrate gastrulation. *Curr. Top. Dev. Biol.* **89**, 163-192.

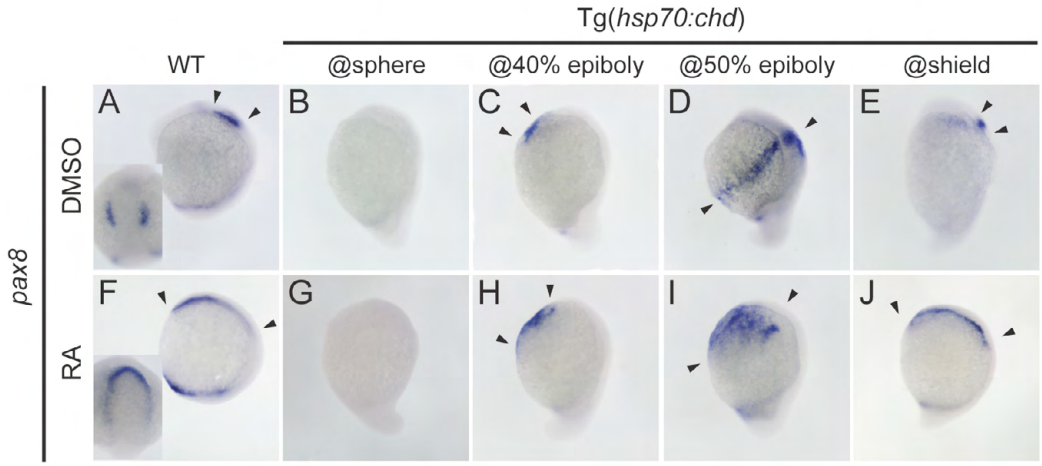

Fig. S1. Anteriorly expanded *pax8*, caused by activation of RA signaling, is patterned by BMP signaling with the same temporal dynamics as the normal posterior domain. (**A-E**) Expression of *pax8* (arrowheads) in wild type (A, *n*=42/42) and in Tg(*hsp70:chd*) heat shocked at sphere (B, *n*=38/38), 40% epiboly (C, *n*=28/31), 50% epiboly (D, *n*=31/35) and shield (E, *n*=30/31) stage. (**F-J**) *pax8* expression in RA-treated wild type (F, *n*=38/39) and RA-treated and heat shocked Tg(*hsp70:chd*) at sphere (G, *n*=30/30), 40% epiboly (H, *n*=31/35), 50% epiboly (I, *n*=32/34) and shield (J, *n*=37/38) stage. Lateral views, dorsal to right with anterior to top, except for insets in A and F, which are dorsal views with anterior to top. All are at the 6-somite stage.

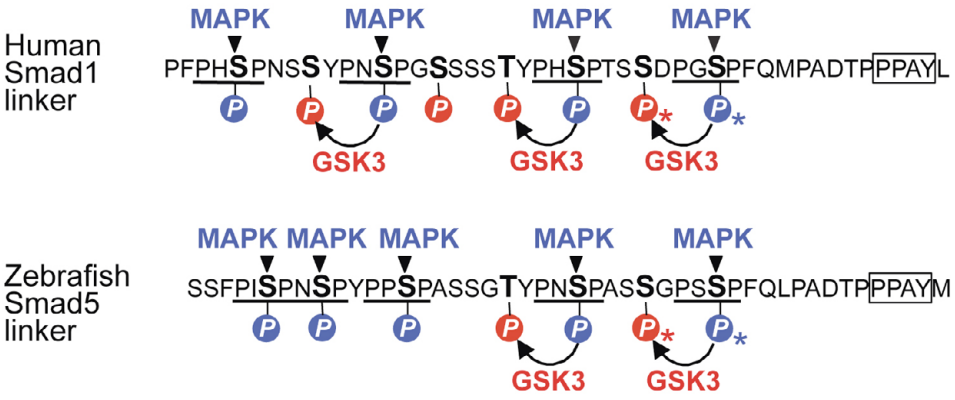

Fig. S2. FGF/MAPK and Wnt/GSK3 phosphorylation sites in the zebrafish Smad5 linker region. Zebrafish Smad5 contains MAPK (blue) and GSK3 (red) phosphorylation sites in its linker region. The box indicates the PPAY binding site of Smurf1 and the asterisks indicate antibody recognition sites for P-Smad1/5^{MAPK} and P-Smad1/5^{GSK3}.

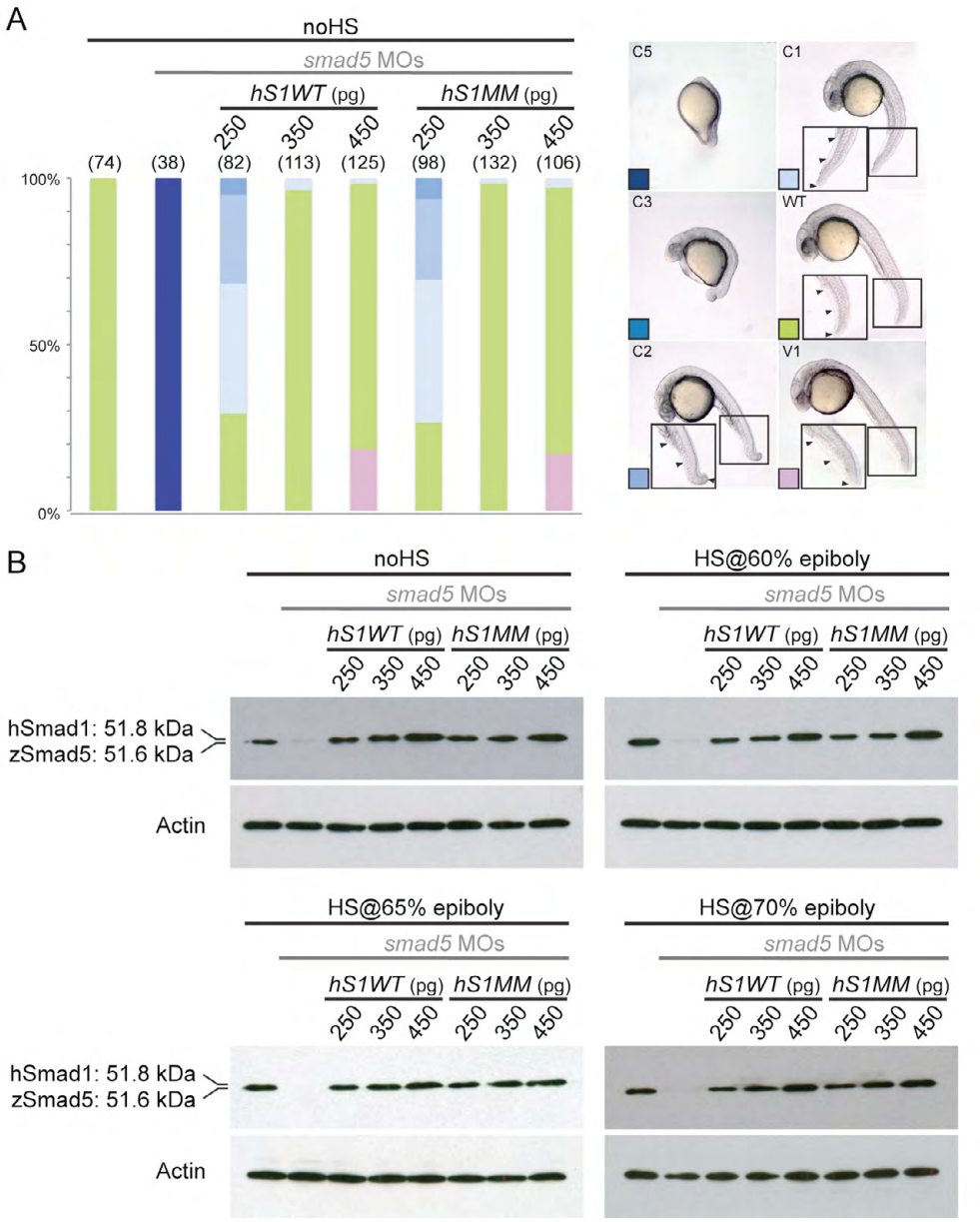

Fig. S3. *hSmad1WT* and *hSmad1MM* mRNAs similarly rescue Smad5-deficient dorsalized embryos and hSmad1WT and hSmad1MM are equally stable in the injected embryos. (**A**) Percentage of embryos that show severely (C5), moderately (C3) and mildly (C1/C2) dorsalized, wild-type (WT) and V1 (diminished eye size and increased ventral tail fin tissue) phenotypes in control and *smad5* MO-injected Tg(*hsp70:chd*) embryos without heat shock, also injected with either *hSmad1WT* mRNA (250, 350 or 450 pg) or *hSmad1MM* mRNA (250, 350 or 450 pg). (**B**) Western blot for total Smad1/5 protein in the same embryos as shown in A. Embryos were collected at 80% epiboly stage. Control and *smad5* MO-injected Tg(*hsp70:chd*) embryos, also injected with *hSmad1WT* mRNA (250, 350 or 450 pg) and *hSmad1MM* mRNA (250, 350 or 450 pg), and either not heat shocked (noHS; upper left panel) or heat-shocked at 60% epiboly (upper right), 65% epiboly (lower left) or 70% epiboly (lower right).

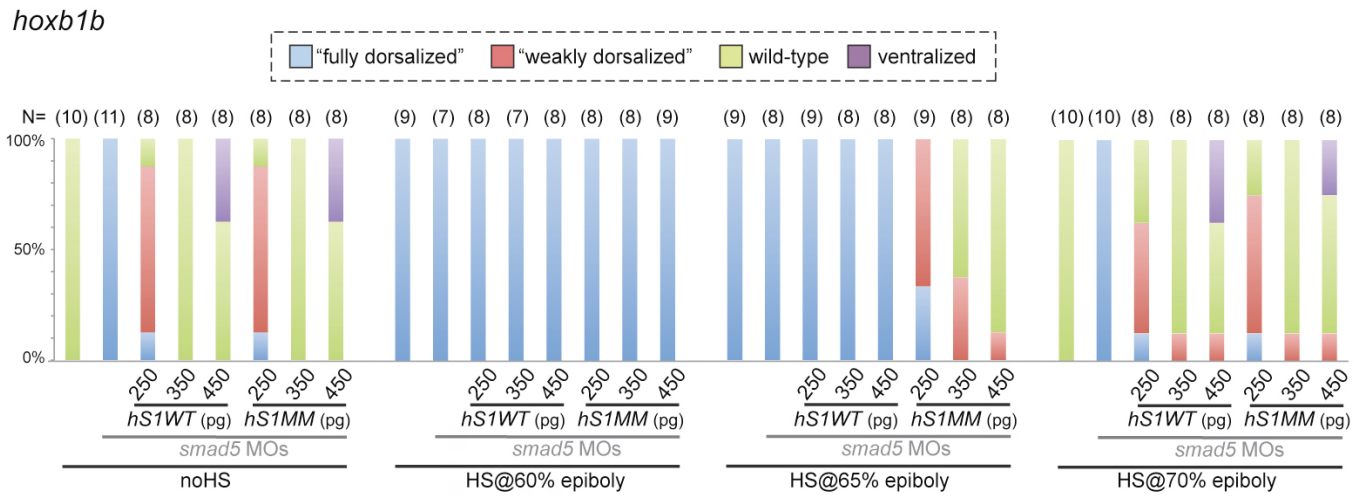

Fig. S4. *hSmad1MM* causes precocious patterning of DV tissues. Percentage of embryos exhibiting a fully dorsalized, weakly dorsalized, wild-type or ventralized phenotype in control and *smad5* MO-injected embryos, also injected with *hSmad1WT* mRNA (250, 350 or 450 pg) and *hSmad1MM* mRNA (250, 350 or 450 pg), and with either no heat shock or heat shocked at different stages to induce expression from Tg(*hsp70:chd*).